Chapter 2
Mathematics of the *Not-So-Solid* Solid Earth

Scott D. King

Abstract As a result of climatic variations over the past 700,000 years, large ice sheets in high-latitude regions of the Earth formed and subsequently melted, loading and unloading the surface of the Earth. This chapter introduces the mathematical analysis of the vertical motion of the solid Earth in response to this time-varying surface loading. The chapter focuses on two conceptual models; the first, proposed by Haskell [Physics, **6**, 265–269 (1935)], describes the return to equilibrium of a viscous half-space after the removal of an applied surface load; the second, proposed by Farrell and Clark [Geophys. J. Royal Astr. Soc., **46**, 647-667 (1976)], illustrates the changes in sea level that occur when ice and water are rearranged on the surface of the Earth. The sea level equation proposed by Farrell and Clark accounts for the fact that sea level represents the interface between two dynamic surfaces: the sea surface and the solid Earth, both of which are changing with time.

Key words: sea level, gravitational potential, Stokes' equation, viscous relaxation

2.1 Ice Ages and Glacial Isostatic Adjustment

For the past 700,000 years, the Earth's climate has alternated between glacial and interglacial conditions, with a periodicity on the order of 100,000 years. A conceptual model emphasizing the roles of orbital variations and atmospheric CO_2 concentration is explored in Chapter **??** of this volume. During glacial periods, lower temperatures result in the growth of large ice sheets at higher latitudes, removing water from the ocean basins and lowering sea levels. During interglacial periods, these large ice sheets melt, returning water stored on land to the oceans, resulting in a relative rise in sea levels. The movement of water in both liquid and solid form be-

Scott D. King
Department of Geosciences, 926 West Campus Drive, Virginia Tech, Blacksburg, VA 24061 USA.
e-mail: sdk@vt.edu

tween continental land masses and ocean basins during the glacial–interglacial cycle creates a time-varying mass load on the surface of the Earth on a time scale that is short compared with the response time of the Earth's surface. The mass of these ice sheets is sufficient to deform the solid Earth, causing subsidence and then, upon subsequent melting of the ice sheet, rebound of the surface. The response of the solid Earth to the time-varying surface load brought about by the waxing and waning of large-scale ice sheets is called *Glacial Isostatic Adjustment* (GIA). Isostasy (or isostatic) is a term used by Earth scientists to describe the Archimedean principle that any object, wholly or partially immersed in a stationary fluid, is buoyed up by a force equal to the weight of the fluid displaced by the object.

During the last great ice age, Scandinavia and North America were covered with thick sheets of ice up to 5 km thick (Figure 2.1.1). In northern Europe, the northward extent of the ice sheet covered Svalbard and Franz Josef Land, and the southern boundary passed through Germany and Poland. In North America, the ice covered most of Canada, extending as far south as the Missouri and Ohio Rivers, and eastward to Manhattan. When the ice sheets melted, the surface of the Earth began to return to its equilibrium elevation (rebound), a process that continues to the present day [21, 22, 38, 40]. The water stored in these ice sheets lowered the sea level glob-

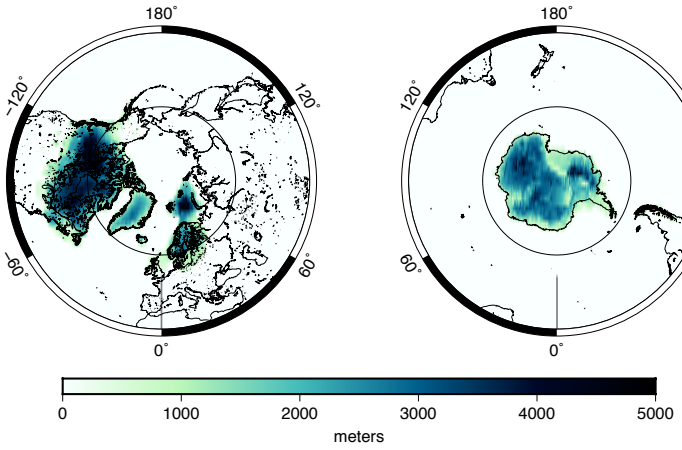

Fig. 2.1.1 Ice thickness 26,500 years before present based on the ICE-6G model [33].

ally by 115–135 meters relative to present-day sea levels [23], and present-day sea levels are at or near the maximum level in the glacial–interglacial cycle.

While water is also present both in the atmosphere and stored as groundwater within the near surface of the Earth, the volumes of water involved in the atmospheric water cycle (e.g., precipitation, evaporation, and transpiration) and stored as groundwater do not vary significantly over the glacial/interglacial time scale.

Changes in these water reservoirs have a much smaller effect on the solid Earth in comparison with the changing mass load of the ice sheets.

2.1.1 Sea Level Changes

Tidal gauges were originally designed to measure the daily and monthly changes in water level due to tides in shallow harbors. A typical tidal gauge would consist of a mechanical float enclosed in a cylindrical well to isolate the float from wind waves. After removing the daily and monthly tidal signals, it is possible to derive a record of the mean sea level from these historical tidal gauge measurements; at some locations, the records are continuous, covering several centuries. Of course, these records are spatially limited to coastal regions, for obvious reasons. It is also necessary to reference a tidal gauge to a local geodetic benchmark, to ensure that the local land surface is stable and that the recorded measurement reflects a change in sea level and not local subsidence or uplift of the land. While still used in some locations, these early gauges have been superseded by pressure, acoustic/ultrasonic, or radar gauges. (Here and throughout the remainder of this chapter, we use the term "sea level" to refer to the level of a hypothetical ocean surface in the absence of wind waves.)

Figure 2.1.2 shows a time series of annual mean sea level anomalies for Amsterdam [42] and Stockholm [7]. (The *sea level anomaly* is the deviation of the actual sea level from some reference level.) The point of this figure is to illustrate the trend as a function of time, and this is not dependent on the specifics of the reference baseline. In Amsterdam, the sea level increased nearly 200 millimeter during the period 1700–1925, while the sea level in Stockholm decreased almost 1000 millimeter between 1770 and 1980. While sea level observations at these locations continue to be

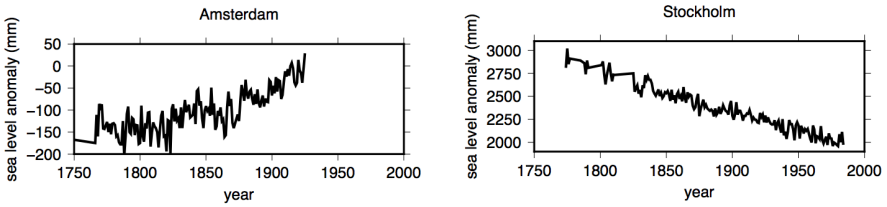

Fig. 2.1.2 Annual mean sea level anomalies for Amsterdam [42] and Stockholm [7]. Data obtained from `http://www.psmsl.org/data/longrecords/`.

recorded, the changes in instrumentation and analysis techniques mean that matching modern tide-gauge measurements with these historical records is a nontrivial exercise. For the purpose here, these historical records are sufficient to illustrate the longer-term trends in the sea-level observations.

The traditional approach to estimating the impact of ice sheets on the sea level assumed that measuring the age of submerged beaches (for example, by radiocarbon dating) in stable areas was sufficient to determine the historical changes in sea level. The assumption was that sea level rise is a global phenomenon and that, just as increasing the water level in a bathtub would increase the water level everywhere, sea level rise at one point would inform the global trend. This allowed researchers to extend the sea-level record further back in time, although with a greater degree of uncertainty. The time series in Figure 2.1.2 present a problem for this traditional approach. Why does the sea level appear to be rising at one location and falling at another? The model described by Farrell and Clark [9], which we will discuss in Section 2.3, illustrates that the distribution of ice and the shape of the surface of the solid Earth play an important role in the analysis of sea-level change.

In any given area, the local sea level is the intersection of two dynamic surfaces: the sea surface and the irregular solid surface, both of which are changing with time. Globally, the sea level is not at a uniform radial distance from the center of the Earth (or some other suitable reference frame) but varies spatially because it follows a surface of equal gravitational potential. While water is removed and added from the ocean basin with the growth and melting of the ice sheets, the gravitational attraction of the ice sheets deforms the ocean surface, thus changing the gravitational potential in the region around the sheet. Also, the change in the mass of both the ocean and the ice sheet as water moves from one to the other creates a time-varying load that deforms the surface of the Earth. As the surface deforms, matter within the Earth is redistributed, the gravitational attraction changes, and the sea level responds in turn. This is the topic that will be analyzed in detail in the remainder of the chapter.

2.1.2 Outline of the Chapter

Following is an outline of the chapter. Section 2.2 contains a review of the classical problem studied by Haskell [11, 12] of a mass load on the surface of a viscous half-space. The analysis yields an estimate of the viscosity of the interior of the Earth, which justifies the assumption that the effects of momentum and rotation on the slow creeping flow in the interior of the Earth can be neglected. Haskell's analysis predicts a uniform rise in sea level everywhere. Section 2.3 focuses on spatial variations of the gravitational potential, following the classical work of Farrell and Clark [9]. The analysis assumes a rigid Earth but allows for a nonuniform sea-level rise. The subsequent Section 2.4 builds on this work by adding elastic deformations to obtain a more realistic model of a solid Earth. Since purely elastic behavior is not consistent with the GIA observations, some degree of viscous behavior is required. The most common model of a viscoelastic medium is the Maxwell rheology model, which is discussed in Section 2.5. The final section, Section 2.6, summarizes the main points of the chapter with references to more in-depth reviews, and describes various open problems.

2.2 The Haskell Problem: Viscous Relaxation of the Solid Earth

It may seem extraordinary that on time scales longer than we can perceive the *terra firma* upon which we go about our daily lives actually behaves like a fluid, albeit a highly viscous fluid. Yet, the study of Earth's tectonic plates shows that the surface of the Earth moves with velocities on the order of tens of millimeters per year [26, 37, 44]—that is, roughly the rate at which human finger nails grow [3]. In addition to the horizontal motions of the Earth's surface, the surface deforms vertically as a result of both imposed surface loads and stresses from within the Earth [4].

The first mathematical formulation of the rebound of the surface of the Earth after the melting of an ice sheet was given by Haskell [11, 12]. Haskell calculated the flow within a semi-infinite, incompressible, viscous half space, subject to an initial periodic surface displacement given by

$$w_m = w_{m0} \cos \frac{2\pi x}{\lambda}. \tag{2.2.1}$$

Here, λ is the wavelength of the initial load. The amplitude of the deformation of the surface is assumed to be much smaller than its wavelength, $w_m \ll \lambda$. The load-induced displacement generates a hydrostatic pressure gradient, which acts to restore the surface of the Earth to the undeformed equilibrium state ($w = 0$).

The equation of *mass conservation* for an incompressible fluid is

$$\nabla \cdot U = 0, \tag{2.2.2}$$

where U is the velocity vector describing the fluid motion. The equation of *momentum conservation* is obtained by applying Newton's second law to the fluid motion and using the assumption that the stress in the fluid is the sum of a pressure term and a viscous term that is proportional to the gradient of the velocity. The resulting equation is the *Navier-Stokes equation*, which describes the dynamics of fluids in many areas of engineering and science,

$$\rho \left[\frac{\partial U}{\partial t} + U \cdot \nabla U \right] = -\nabla p + \eta \nabla^2 U. \tag{2.2.3}$$

Here, ρ is the density of the fluid, p the pressure, and η the viscosity; $\frac{\partial \cdot}{\partial t}$ is the partial derivative with respect to time.

The viscosity is a measure of the resistance of the fluid to gradual deformation by shear stress; honey is more resistant to flow than water, so honey has a larger viscosity than water. In the SI system of units, viscosity is measured in Pascal-seconds (Pa-s). The viscosities of some common fluids are listed in the adjacent table.

Fluid	Density (kg/m^3)	Viscosity (Pa-s)
Air	1.3	10^{-5}
Water	1000.	10^{-3}
Olive Oil	916.	0.1
Honey	1450.	10
Glacial Ice	800-900	10^{15}

While it may not be obvious that the solid interior of the Earth deforms, consider the movement of glaciers. Glaciers are sometimes called "rivers of ice," and they actually flow in response to gravity acting on their own mass. The rate of glacial motion ranges from less than a meter per year to as much as 30 meters per day when the base of the glacier is decoupled from the underlying bedrock by soft sediments and meltwater.

For specific problems, it is often possible to simplify the Navier–Stokes equation because one or more terms in the equation are significantly smaller than the others. To show this, it is helpful to rewrite the equation in terms of dimensionless variables, which are of order 1, multiplied by a dimensional scaling constant. For example, length can be written as $x = x'L$, where x' is of order 1 and L represents the characteristic length scale of the problem. In the problem under consideration, the length scale is the wavelength of the applied load, λ. Similarly, the depth can be written as $y = y'L$, using the same length scale of the problem, L. The velocity can be rewritten as $U = U'U_0$, where U_0 is the characteristic velocity of the problem. Here, the velocity of Earth's tectonic plates serves as a reasonable estimate of the characteristic velocity, $U_0 = 0.01$ m/yr, or $U_0 \approx 3.16 \times 10^{-9}$ m/s. (Even though the second is the unit of time in the SI system, geoscientists think of plate velocities in millimeters per year. There are approximately $\pi \times 10^7$ seconds in a year.) The characteristic time can now be defined in terms of L and U_0, $t = t'L/U_0$. A logical choice for pressure scaling is $p = p'\eta U_0/L$, which results in units of Pascals, the SI unit of pressure.

Substituting the above relationships into Eq. (2.2.3), we obtain the Navier–Stokes equation in dimensionless form,

$$Re\left[\frac{\partial U'}{\partial t'} + U' \cdot \nabla' U'\right] = -\nabla' p' + (\nabla')^2 U', \tag{2.2.4}$$

where the scaling constants and properties of the fluid have been grouped into a single term, the *Reynolds number*,

$$Re = \frac{\rho U_0 L}{\eta}. \tag{2.2.5}$$

The units in the Reynolds number cancel, so Re is a dimensionless quantity—one of several that arise in the study of fluid mechanics. It is also noteworthy that the primed equation (2.2.4) is dimensionless. This is useful for a variety of reasons; for example, if the physical properties of different problems result in the same Reynolds number, their solutions will be identical. Hence, if the characteristic length is increased by a factor of 10, the dimensionless solution will be the same if the viscosity is also increased by a factor of 10. The dimensional solution can be recovered by multiplying the dimensionless solution by the scaling constants.

While nothing has been said yet about the viscosity of the interior of the Earth, it is not hard to imagine that it is large, at least as large as the viscosity of glacial ice; hence, the Reynolds number will be very small, and the terms on the right-hand side of the Navier-Stokes equation can be ignored. This assumption will be

checked after the final solution has been obtained. Following the same procedure, it is easy to show that the terms representing the effects of the Earth's rotation are similar in magnitude to the momentum terms on the left-hand side of the Navier–Stokes equation. Thus, if our analysis shows that momentum can be ignored, so can rotation.

Consider a two-dimensional domain in a vertical plane. Choose a Cartesian coordinate system in the plane, with horizontal coordinate x and vertical coordinate y, with y increasing downwards. The surface of the Earth is represented by a function $y = w(x)$. Let u and v denote the x and y components, respectively, of the velocity vector U.

The components of Eq. (2.2.4) in the x and y direection are

$$-\frac{\partial p}{\partial x} + \eta\left(\frac{\partial^2 u}{\partial x^2} + \frac{\partial^2 u}{\partial y^2}\right) = 0, \tag{2.2.6}$$

$$-\frac{\partial p}{\partial y} + \eta\left(\frac{\partial^2 v}{\partial x^2} + \frac{\partial^2 v}{\partial y^2}\right) = 0. \tag{2.2.7}$$

This set of equations can be solved using the stream-function formulation [2]; a step-by-step solution can be found, for example, in [14]. In two dimensions, the stream function, $\psi(x,y,t)$, is a scalar whose partial derivatives are related to the components of the velocity,

$$u = \frac{\partial \psi}{\partial y}, \quad v = -\frac{\partial \psi}{\partial x}. \tag{2.2.8}$$

Note that, by construction, $U = (u,v)$ satisfies the equation of mass conservation (2.2.2).

Because the initial displacement of the surface varies in x with a functional form $\cos(2\pi x/\lambda)$, the stream function will vary with a functional form $\sin(2\pi x/\lambda)$. By taking the derivative of Eq. (2.2.6) with respect to y and the derivative of Eq. (2.2.7) with respect to x and subtracting the two resulting equations, we eliminates the pressure. Then, upon substitution of the expressions (2.2.8) we obtain a single biharmonic equation for the scalar ψ. Separating ψ into a function that varies only in x (i.e., $\sin(2\pi x/\lambda)$) and a function that varies only in $Y(y)$, we find that the stream function must have the form

$$\psi = \sin\left(\frac{2\pi x}{\lambda}\right)\left[(A+By)e^{-2\pi y/\lambda} + (C+Dy)e^{2\pi y/\lambda}\right], \tag{2.2.9}$$

where A, B, C, and D are constants, to be determined by the boundary conditions. The constants C and D must be zero because the components of the velocity field must remain finite as the depth of the half space (y) goes to infinity. Differentiating ψ, the components of velocity are

$$u = \sin\left(\frac{2\pi x}{\lambda}\right)\left[\frac{2\pi}{\lambda}(A+By) - B\right]e^{-2\pi y/\lambda}, \tag{2.2.10}$$

$$v = \cos\left(\frac{2\pi x}{\lambda}\right)\frac{2\pi}{\lambda}(A+By)\,e^{-2\pi y/\lambda}. \tag{2.2.11}$$

The shear tractions exerted on the solid Earth by the atmosphere are negligible, so the horizontal velocity of the flow in the solid Earth is zero at the deformed surface—that is, at $y = w(x)$. Since the displacements of the solid Earth (at most hundreds of meters) are small compared to the size of a typical ice sheet (a thousand kilometers or more), we may assume that $w \ll \lambda$ and apply the boundary conditions at the equilibrium surface—that is, at $y = 0$—instead. Johnson and Fletcher [14] show how to apply the boundary conditions to the deformed surface when w is not small; their solution reduces to the one presented here in the case of small deformations. Setting $u = 0$ at $y = 0$ yields $B = 2\pi A/\lambda$.

To find A, the hydrostatic pressure resulting from the topography ($-\rho g w$, where g is the acceleration due to gravity) is set equal to the normal stress generated by the flow at the surface ($p - 2\mu\frac{\partial v}{\partial y}$), where ρ is the density of the mantle),

$$-\rho g w = p - 2\mu\frac{\partial v}{\partial y}. \tag{2.2.12}$$

The pressure at $y = 0$ can be found by substituting Eqs. (2.2.10) and (2.2.11) into Eq. (2.2.6) and integrating,

$$p|_{y=0} = 2\mu A\left(\frac{2\pi}{\lambda}\right)^2 \cos\left(\frac{2\pi x}{\lambda}\right). \tag{2.2.13}$$

Because $\frac{\partial v}{\partial y}|_{y=0} = 0$, Eq. (2.2.12) reduces to

$$w = -\frac{2\mu A}{\rho g}\left(\frac{2\pi}{\lambda}\right)^2 \cos\left(\frac{2\pi x}{\lambda}\right). \tag{2.2.14}$$

The key step is to substitute Eq. (2.2.11) (with $B = 2\pi A/\lambda$) into Eq. (2.2.14) and recognize that the vertical velocity at the surface is the derivative of the displacement with time, $v = dw/dt$ (at $y = w$). Once again, because the displacements are small compared with the size of a typical ice sheet, we apply this condition at $y = 0$,

$$v|_{y=0} = \left.\frac{dw}{dt}\right|_{y=0} = A\frac{2\pi}{\lambda}\cos\left(\frac{2\pi x}{\lambda}\right) = -w\frac{\lambda g\rho}{4\pi\mu}. \tag{2.2.15}$$

Upon integration, we obtain the expression for w,

$$w(t) = w_{m0}\exp\left(-\frac{\lambda g\rho}{4\pi\mu}t\right). \tag{2.2.16}$$

Hence, the surface of the Earth decays to an equilibrium position as the "fluid" mantle flows from regions of elevated topography to regions of low topography. The grouping of constants $\frac{4\pi\mu}{\lambda g\rho}$ has units of time and is the characteristic time scale of the Glacial Isostatic Adjustment (GIA)—that is, the time it takes the topography to decay by $1/e$. Using reasonable values for the density of the solid Earth, $\rho = 3,300$ kg m^{-3}, the acceleration due to gravity, $g = 10$ m s^{-2}, and the spatial scale of the ice sheet, $\lambda = 1,000$ km, matching the time scale of GIA from the tide-gauge and beach data requires the viscosity of the mantle to be on the order of $\eta \sim 10^{21}$ Pa-s. This is sometimes referred to as the *Haskell value of mantle viscosity* and is an average or effective value, as it assumes that the Earth is a homogeneous fluid. Using the same values of $\rho$and λ, taking $u = 0.01$ m yr^{-1} and the Haskell value of viscosity, $\eta = 10^{21}$ Pa s, we obtain a Reynolds number on the order of 10^{-21}, which justifies the initial assumption that the inertial terms in the Navier-Stokes equation can be ignored.

While the Haskell problem is simplified, the characteristic time of GIA, $\frac{4\pi\mu}{\lambda g\rho}$, is approximately 12,000 years. The last glacial maximum (i.e., the time when the ice sheets were at their largest spatial extent) occurred approximately 26,500 years ago and the North American and European ice sheets began to retreat about 20,000 years ago. The characteristic time predicts that vertical rebound of the Earth's surface should still be continuing—a prediction that has been validated with high-precision GPS observations [13, 21, 22, 27, 29, 38, 40]. Other independent geophysical constraints on mantle viscosity are broadly consistent with the Haskell result [16]. Until recently, observations of vertical uplift were measured almost exclusively along coast lines via sea- and lake-level changes, requiring climatic, hydrographic, and tectonic corrections, and horizontal motions could not be accurately observed at all. This state of affairs changed with the development of high-precision GPS.

2.3 Gravitational Potential: The Spatial Variability of Sea Level

One might assume that estimating the change in sea level is as simple as estimating the mass of ice sheets at their maximum extent, converting this mass to an equivalent volume of water, and adding that volume of water to the ocean. This approach predicts that sea level should have risen by an equal amount everywhere, which is inconsistent with the observations [22, 34], as shown, for example, in the time-series of Figure 2.1.2. Two effects are missing: First, there is a gravitational attraction between the ocean and ice sheets, and second, both the ocean and the ice sheets deform the Earth's surface. Sea level is the intersection of these two dynamic surfaces (the sea surface and the solid Earth surface), both of which are changing with time.

To illustrate the role of gravitational attraction on sea level, consider the simplified problem of a rigid sphere that is initially covered by a thin ocean of uniform depth. This problem is discussed in Farrell and Clark [9], and the text below follows their derivation. We will simplify the problem further by assuming that the ocean has zero density, yet is at the same time in gravitational equilibrium (which

assumes that the ocean has a nonzero density). While these assumptions are clearly inconsistent, they allow for an analytic solution of the problem.

For a spherically symmetric Earth, where r is the distance between the observer and the Earth's center of mass, the gravitational potential is

$$V(r) = \frac{GM_E}{r}, \tag{2.3.1}$$

where G is Newton's gravitational constant and M_E is the total mass of the Earth (which includes the solid Earth and the ocean). Equation (2.3.1) is valid for $r \geq a$, where a is the radius of the Earth. A direct result of the spherical symmetry of the problem is that the sea level of this uniform-depth ocean will be equal to a everywhere, because the gravitational potential at the surface, $V(a)$, is a constant. Now suppose that an ice sheet of mass M_I is extracted from the surface at $r = a$ and placed at a single point on the Earth's surface. Let θ measure the angular distance between the point mass (ice sheet) and an observer. Then the new gravitational potential field is

$$V^I(r,\theta) = \frac{G(M_E - M_I)}{r} + \frac{GM_I}{\sqrt{r^2 + a^2 - 2ar\cos\theta}}. \tag{2.3.2}$$

The superscript ^{I} denotes the combined potential of the Earth plus ice sheet. Note that $M_E - M_I$, and therefore the first term in Eq. (2.3.2), is still spherically symmetric; however, $V^I(a,\theta)$ is a function of θ and therefore $r = a$ is no longer the sea level because $V^I(a,\theta)$ is not constant. Defining a new surface at $r = a + \varepsilon$, where $V^I(a+\varepsilon,\theta) = V^I(a)$ and assuming that $M_I \ll M_E$, it follows that $\varepsilon \ll a$ and a first-order Taylor expansion can be used to approximate $V^I(a+\varepsilon,\theta)$,

$$V^I(a+\varepsilon,\theta) = V^I(a,\theta) + \varepsilon\frac{\partial V^I(a,\theta)}{\partial r}. \tag{2.3.3}$$

It is sufficiently accurate to use the approximation $\frac{\partial V^R(a,\theta)}{\partial r} = -g$, where g is the acceleration due to gravity at the Earth's surface. Rearranging Eq. (2.3.3) and substituting $g = \frac{GM}{a^2}$, we obtain

$$\varepsilon(\theta) = \frac{M_I a}{M_E}\left(\frac{1}{2\sin(\theta/2)} - 1\right). \tag{2.3.4}$$

At this point, the analysis has yet to account for the volume of water that has been lost from the ocean; therefore, $V^I(a+\varepsilon(\theta),\theta)$ is constant but is not the sea level. To account for the reduced ocean volume, recall that if $a+\varepsilon(\theta)$ is an equipotential surface, then for any constant $c \ll a$, $a+\varepsilon(\theta)+c = a+\varepsilon_2(\theta)$ is also an equipotential surface. The trick is to choose a value of c so as to conserve the total mass of the system. Farrell and Clark suggest that the result thus obtained is an accurate estimate of sea level.

To calculate c, note that the volume between the surfaces a and $a+\varepsilon$ integrated over the sphere is zero, so in order to conserve mass, it must be the case that

$$\int_0^{\pi} 2\pi\rho_w c a^2 \sin\theta \, d\theta + M_I = 0, \tag{2.3.5}$$

where ρ_w is the density of sea water. Solving Eq. (2.3.5) for c and using $M_E = (4/3)\pi a^3 \rho_E$, where ρ_E is the mean density of the Earth, we obtain

$$\varepsilon_2(\theta) = \frac{M_I a}{M_E}\left(\frac{1}{2\sin(\theta/2)} - 1 - \frac{\rho_E}{3\rho_w}\right). \tag{2.3.6}$$

The first two terms on the right-hand side represent the distortion of sea level due to the gravitational attraction of the ice; the third term is the uniform fall in sea level due to the removal of a volume of water equivalent to the ice mass M_I from the oceans. Figure 2.3.1 shows the change in sea level (normalized by the predicted uniform sea-level drop) due to the removal of an amount of water equivalent to M_I as a function of the angular distance from the ice mass.

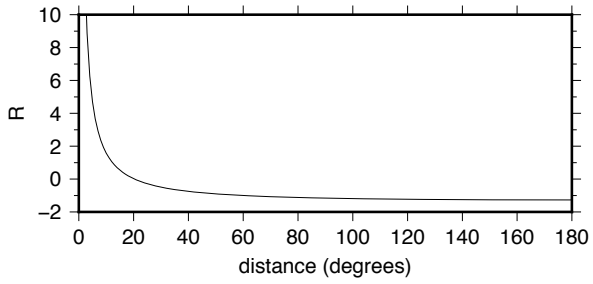

Fig. 2.3.1 The normalized change in sea level as a function of distance from the ice mass for a rigid Earth, including the effect of the gravitational attraction of the ice sheet.

At a point 60° from the ice mass, the predicted sea-level drop is the same as predicted from the uniform sea-level decrease. Beyond 60°, the sea-level drop is greater than the uniform prediction, while within 20° of the ice load the sea level actually rises due to the gravitational attraction of the ice acting on the ocean. This result provides a qualitative explanation for the historical sea-level trends observed at Amsterdam and Stockholm shown in Figure 2.1.2: Stockholm is closer to the center of the Fennoscandian ice sheet than Amsterdam. However, a word of caution is appropriate here, because the assumptions made in this section may limit the applicability of the results. Nonetheless, it is instructive as an illustration of the role of the gravitational attraction of the ice sheet on sea level.

The problem described here considers the shoreline to be spatially fixed with time as the sea level rises and falls during a glacial cycle. Or to help the reader visualize, it is equivalent to assuming that the edges of the ocean basins are characterized by steep cliffs that prevent the water from moving either landward or oceanward.

More accurate and complex shoreline calculations are described and compared in Mitrovica and Milne [24].

2.3.1 Extending the Solution to an Irregular Ice Distribution

To extend the point-mass problem to any arbitrary volume of ice, Eq. (2.3.6) is convolved with a function that represents the variation in ice thickness, $I(\theta', \phi')$. The change in sea level, $S(\theta, \phi)$, due to a change in ice mass is given by the integral

$$S(\theta,\phi) = \iint\limits_{ice} \left[\frac{a}{M_E} \left(\frac{1}{2\sin(\alpha/2)} - 1 - \frac{\rho_E}{3\rho_w} \right) \right] \rho_I I(\theta',\phi') a \sin(\theta') \, d\theta' \, d\phi', \tag{2.3.7}$$

where α is the arc length between a point (θ, ϕ) on the ocean and the location (θ', ϕ') of the ice. The term in brackets, which is identical to (2.3.6) with unit ice mass (M_I), is the Green's function for this problem.

To account for the gravitational attraction of the mass of the ocean on sea level, one can similarly convolve the Green's function with sea level. An iterative solution strategy for this problem is discussed in Farrell and Clark [9].

2.4 Deformation of the Solid Earth: The Elastic Earth

While the analysis in Section 2.3 is instructive and provides a possible qualitative explanation for the trends observed in the sea-level curves shown in Figure 2.1.2, the results of Section 2.3 are inconsistent with the Haskell problem in Section 2.2 because the Earth was assumed to be rigid. In this section we will outline how the sea-level equation, Eq. (2.3.7), can be extended to include the deformation of the solid Earth. First, it is necessary to briefly review the possible ways in which the solid Earth might deform.

When placed under a load, the surface of the Earth exhibits both elastic and viscous behavior. A material is said to behave elastically when it deforms instantaneously in response to an applied force and returns to its original state immediately after the force is removed. A spring is often used as the classic example of elastic behavior. On the other hand, a viscous material undergoes transient, permanent deformation when a force is applied. Honey is often used as the classic example of a viscous fluid. A material that behaves both elastically and viscously is called a *viscoelastic material*. A viscoelastic material will experience both instantaneous and transient deformation upon the application of a force. When the original force is removed, the transient deformation is reversed; however, unlike the elastic material, the viscoelastic material does not return to it's initial state and some permanent deformation is retained. The child's toy Silly-Putty is often used as an example of a viscoelastic material. When Silly-Putty is dropped, it bounces like a rubber ball,

exhibiting elastic behavior in response to the short-timescale force of the Silly-Putty and accelerating due to the force of gravity as it falls, until it is stopped by the immovable floor. If a similar force is applied over a longer time period, the Silly-Putty yields and stretches into a long thin strand, much like taffy.

The Earth also exhibits this dual deformation behavior depending on the time scale of the forcing function. Over the time period of several million years, Earth's surface deforms viscously when subjected to an applied load such as the mass of a volcano or the volume of water in the ocean basin [8]. This is the mode of deformation that Haskell assumed to be appropriate in the problem described in Section 2.2. On a time scale of seconds to hours, the Earth behaves elastically in response to seismic waves. Since the time scale of the growth and decay of ice sheets is on the order of 100,000 years, elastic deformation cannot be ignored [22, 45]. The derivation of the elastic response of an incompressible spherically symmetric Earth is given in [1, 5, 9]. Here, we focus on how the sea-level equation (2.3.7) can be modified to account for the deformation of the Earth.

The solution of the elastic deformation problem requires solving the linear momentum equation (similar to the Navier–Stokes equation for viscous flow) for the displacement (instead of the velocity as in the viscous flow problem), coupled with the solution of a Poisson equation for the gravitational potential of a spherically symmetric body with material properties that are functions only of the radius, subject to a disk-shaped surface boundary load. The elastic deformation of a spherical body subject to a disc point load can be represented in terms of three *Love numbers*, h_l, k_l, and l_l, which depend only upon the radius, r, and the degree of the spherical harmonic, l [20].

A short digression here is necessary to introduce spherical harmonics. Spherical harmonics are often used to represent functions on a sphere. They play the same role on a sphere as sines and cosines on a line; as such they appear frequently in geophysical problems. With the proper normalization, spherical harmonics can be written in terms of Legendra polynomials, $P_{lm}(\cos\theta)$, multiplied by cosines and sines in the azimuth ϕ,

$$Y_{lm}(\theta,\phi) = P_{lm}(\cos\theta)(C\cos m\phi + S\sin m\phi), \tag{2.4.1}$$

where l is the spherical harmonic degree and m is the spherical harmonic order. The spherical harmonic functions form a set of basis functions on a sphere, so they can be used to represent any function on a sphere with an infinite set of coefficients, with many similarities between spherical harmonics and Fourier series analysis in terms of solution techniques. For example, if the topography of a planet is given by $\mathrm{topo}(\theta,\phi)$, then

$$\mathrm{topo}(\theta,\phi) = \sum_{l=0}^{\inf}\sum_{m=-l}^{l} T_{lm}Y_{lm}(\theta,\phi), \tag{2.4.2}$$

where the coefficients T_{lm} are independent of θ and ϕ. The spherical harmonic functions, normalized so that their integral over the sphere is one, for degrees 1 through 4 are plotted in Figure 2.4.1. Spherical harmonics of order zero ($m = 0$) are only func-

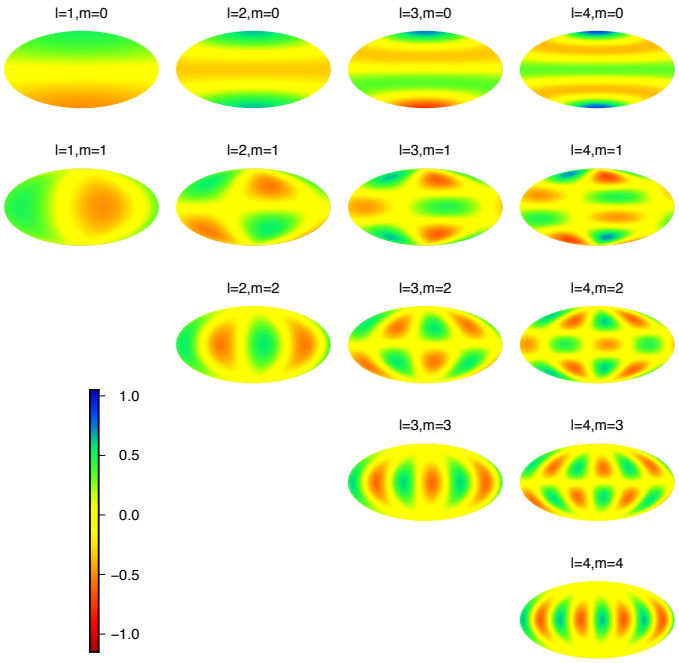

Fig. 2.4.1 Plots of normalized spherical harmonics for degree and orders 1 through 4.

tions of latitude; they are often called zonal harmonics. Spherical harmonics with equal degree and order ($l = m$) are only functions of longitude; they are often called sectoral harmonics, because their pattern resembles the sections of an orange. The other harmonics are simply called mixed harmonics.

Two practical rules of thumb, which are useful when thinking about spherical harmonics: $P_{lm}(\cos\theta)$ has $(l-m)$ zero crossings between the North and South pole, while $\cos(m\phi)$ has $2m$ zero crossings between $0 \leq \phi \leq 2\pi$. Thus, when thinking about scaling properties represented in spherical harmonics on the surface of the Earth (6,371 km), $\frac{2\pi \cdot 6{,}371}{l-m} \approx \frac{40{,}000}{l-m}$ km, and for longitude, $\frac{2\pi \cdot 6{,}371}{m} \approx \frac{40{,}000}{m}$ km.

Returning to the elastic response of a spherical body subject to a disc point load, we note that each set of boundary conditions defines a distinct Green's function and, thus, a different triplet of Love numbers. While the determination of the Love numbers is beyond the scope of this chapter (see [1, 5, 9, 20] for details), the Love numbers have a straight forward interpretation. If V_l is a single term in the spherical harmonic expansion of the gravitational potential V with a perturbation of degree l, then $k_l V_l$ is the gravitational potential due to the elastic deformation within the Earth. In the spherically symmetric elastic deformation problem, the solution is comprised of only the zonal spherical harmonics ($m = 0$). Thus, the perturbation in the gravitational potential of degree l on the surface is the sum of the perturbation due to the

applied mass, V_l, and the perturbation due to the new arrangement of matter within the Earth, $k_l V_l$. The quantity $h_l V_l/g$ is the radial displacement of the solid surface away from the reference spherical surface, $r = a$. When $h_l V_l/g$ is positive, the radius of the Earth's solid surface after the deformation is greater than the original radius a, and when $h_l V_l/g$ is negative, the radius the Earth's solid surface after the deformation is smaller than the original radius a. The Love number l_l, is related to tangential displacements and is not relevant to the vertical load problem.

To apply the Love numbers to the sea-level equation, starting with equation (2.3.2), the gravitational potential is expanded in terms of Legendre polynomials,

$$V(r,\theta) = \frac{a\,g}{M_E}\sum_{l=0}^{\infty}\left(\frac{a}{r}\right)^{l+1} P_l(\cos\theta), \tag{2.4.3}$$

where the P_l is the Legendre polynomial of order l. At the surface ($r = a$), the infinite series has the finite sum,

$$\sum_{l=0}^{\infty} P_l(\cos\theta) = \frac{1}{2\sin(\theta/2)}, \tag{2.4.4}$$

which implies the equivalence of Eqs. (2.3.2) and (2.4.3). While Eq. (2.4.4) is at first not obvious, it follows from the Legendra polynomial generating function,

$$\sum_{l=0}^{\infty} x^l P_l(\mu) = \frac{1}{(1-2\mu x+x^2)^{1/2}}, \tag{2.4.5}$$

with $x = 1$, $\mu = \cos\theta$, and the trigonometric identity $\sin(\theta/2) = \sqrt{(1-\cos\theta)/2}$.

For each spherical harmonic degree l, $(1+k_l)V_l$ is the perturbation potential on the spherical surface $r = a$ and $h_l V_l/g$ is the displacement of the solid boundary with respect to the reference surface, $r = a$. It follows that the perturbed gravitational potential on the displaced boundary of the solid Earth is $V_l^E = (1+k_l+h_l)V_l$, because $-g(h_l V_l/g)$ is the change in the gravitational potential that occurs when moving from the reference surface ($r = a$) to the newly deformed boundary. The Green's function for the elastic problem can therefore be represented by

$$V_l^E = \frac{ag}{M_E}\sum_{l=0}^{\infty}(1+k_l+h_l)\,P_l(\cos\theta), \tag{2.4.6}$$

and the solution for the sea level proceeds following the approach described for the rigid Earth in Section 2.3 [9].

2.5 Deformation of the Solid Earth: The Maxwell Rheology

While Section 2.4 illustrates the solution to the sea-level equation for a purely elastic Earth, elastic deformation is not consistent with the GIA observations. When

the deforming force is removed, an elastic material instantaneously returns to the equilibrium state; therefore, the elastic deformation model predicts that the Earth's surface would have returned to the equilibrium state as the ice sheets melted and today no deformation due to GIA should be expected. Hence, some degree of viscous behavior is required to explain the GIA observations.

While there are several possible models for viscoelastic materials, the *Maxwell rheology model* is the one that is predominantly used in GIA studies. In the context of Maxwell rheology, the sea-level equation becomes time dependent.

Figure 2.5.1 shows a simple representation of a Maxwell solid as a purely viscous damper connected in series with a purely elastic spring. Under an applied axial

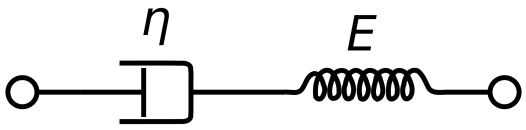

Fig. 2.5.1 The Maxwell rheology model, a linear spring and viscous dashpot in series.

stress, the total stress, σ_{Total}, and the total strain, $\varepsilon_{\text{Total}}$, are defined as follows:

$$\sigma_{\text{Total}} = \sigma_D = \sigma_S, \tag{2.5.1}$$

$$\varepsilon_{\text{Total}} = \varepsilon_D + \varepsilon_S. \tag{2.5.2}$$

The subscript D refers to the damper (viscous deformation), the subscript S to the spring (elastic deformation). Taking the derivative of strain with respect to time, we obtain

$$\frac{d\varepsilon_{\text{Total}}}{dt} = \frac{d\varepsilon_D}{dt} + \frac{d\varepsilon_S}{dt} = \frac{\sigma}{\eta} + \frac{1}{E}\frac{d\sigma}{dt}, \tag{2.5.3}$$

where E is the elastic modulus and η the viscosity.

Calculating sea-level changes on a viscoelastic Earth requires a Green's function for the perturbation to the gravitational potential, which depends on both the distance from a point mass and the time that has elapsed since the mass was applied to the Earth's surface. The Green's function contains all the necessary information relating to the rheological structure of the Earth. Green's functions for a range of Maxwell Earth models were determined by Peltier [32], who used the correspondence principle in conjunction with classical elastodynamics.

2.6 Discussion

While there has been significant progress in understanding the response of the solid Earth and sea level due to changes in the distribution of ice and water over the

surface of the Earth, challenges remain. A comprehensive overview of the processes that affect sea level can be found in a recent article by Cazenave and Nerem [6]. Other factors that could affect sea-level changes can be grouped into four broad categories: 1) changes in the volume of the ocean basin as the result of a change in the topography of the ocean floor; 2) changes in the shape of the gravitational potential; 3) local subsidence or uplift of the land-sea interface; and 4) changes in the total volume of water in the ocean basin. We briefly discuss some details of each category.

Changes in the volume of the ocean basin. A change in the volume of the ocean basin will occur when tectonic plates reorganize or when there is a change in the velocity of an oceanic plate. This is because the ocean-floor topography, which geoscientists call *bathymetry*, is controlled by the conductive cooling of the oceanic plates [30]. A half-space that cools due to conduction has a square-root of time functional form. Parsons and Sclater [30] show that ocean bathymetry should increase with the square root of age of the ocean flow, where the new crust that forms at a mid-ocean ridge defines time zero. If the ocean plate moves away from a mid-ocean ridge faster, then the bathymetry will be shallower at a fixed distance from the ridge. If the ocean plate moves slower, then the bathymetry will be deeper at the same distance. Thus, if the velocity of an oceanic plate increases, the volume of the ocean will decrease (over time) and sea level will increase (all other factors being equal), while if the velocity of an oceanic plate decreases, the volume of the ocean will increase and sea level will fall. This change in shape of the sea floor changes on a time scale of millions to tens of millions of years, significantly longer than the time scale of GIA, and does not impact current estimates of sea level.

Changes in the shape of the gravitational potential. A change in the shape of the gravitational potential is controlled by the time scale of the redistribution of mass. The distribution of ice/water on the surface of the Earth (Section 2.3) is already included in the GIA analysis. On the other hand, the erosion of rock by ice sheets, which generates material that is then incorporated into the ice and subsequently deposited as the ice melts, is not accounted for in current GIA models. Ice sheets transport eroded material away from the center of glaciation to the continental shelf edge, where it is deposited in a series of fans. Nygård et al. [28] estimate that 32,000 km^3 of sediment have been deposited on the North Sea Fan off the west coast of Norway over the last 450 Myr. This time span is significantly longer than the glacial–interglacial cycle, so the accumulation of sediment from a single glacial–interglacial cycle is probably significantly less. Even so, the total mass of sediment is small compared to the estimate of 5×10^6 km^3 of ice that was loaded onto (and then removed from) the Fennoscandian platform in a period of roughly 100,000 years [18]. The effects of other changes such as anthropogenic groundwater pumping or climate-related processes have been shown to be small compared with the GIA signal [35, 19].

Local subsidence or uplift of the land-sea interface. Local subsidence and uplift of the land surface that are not due to GIA are monitored by carefully tying the tide-gauge measurements into a global geodetic reference frame. In this regard, the

development of high-precision GPS measurements has significantly reduced one of the major sources of uncertainty in the GIA observations. In addition, because GPS can measure uplift and horizontal motions over land, this has significantly expanded the range of GIA observations [13, 21, 22, 27, 29, 38, 40].

Changes in the total volume of water in the ocean basin. One of the effects of anthropogenic climate change is that the large ice sheets over Greenland and Antarctic are melting at increasingly faster rates. The resulting changes in sea level have been shown to possess a unique pattern indicating where the most active melting is currently taking place [25, 41]. This melting will change the volume of water in the ocean basin and will change the shape of the gravitational potential because of the redistribution of the ice/water, following the same logic as described in Section 2.3. In principle, this can be modeled with the same analysis used to study the longer-time scale processes associated with the melting of glacial–interglacial ice sheets. The challenge is unraveling the ongoing effect of GIA from the last glacial cycle with the present–day changes in ice/water due to current melting of the Greenland and Antarctic ice sheets.

Two significant areas of uncertainty in the analysis of GIA observations are the distribution of ice at the last glacial maximum [33] and the rheology of the mantle [16]. Mantle rheology impacts not only the response of the surface to imposed surface loads such as ice and water, but also controls the motion of the tectonic plates [10] and regulates the heat flow from within the Earth by controlling the vigor of convection within the solid Earth [36]. While the viscosity of minerals that make up the mantle is strongly dependent on temperature and pressure and could vary with grain size and strain rate, depending on the deformation mechanism [16], many GIA studies focus on depth-dependent viscosity profiles. While viscosity models other than depth-dependent models have been considered [31, 39, 43, 45], the primary control on vertical surface motion is from depth-dependent rheology, which is by far the rheology that has been given the most attention. Lateral variations in rheology are likely to be most prevalent at the boundary between continents and oceans [15, 17], which is where the sea-level observations are made.

The ongoing deformation of the solid Earth and the associated change in sea level in response to the glacial cycle are challenging interdisciplinary problems with a strong historical connection to the mathematical community. Advancing our understanding would benefit from new data assimilation and modeling strategies, improvements in viscoelastic modeling, a better understanding of mantle rheology, and a more complete understanding of present-day changes in ice load.

Acknowledgements The author acknowledges support from NSF Grant EAR-1250988.

References

1. Backus, G.E.: Converting vector and tensor equations to scalar equations in spherical coordinates. Geophys. J. **13**, 71–79 (1967)
2. Batchelor, G.K.: An Introduction to Fluid Dynamics. Cambridge University Press, Cambridge UK (1967)
3. Bean, W.B.: Nail growth. Thirty-five years of observation. Arch Intern. Med. **140**, 73–76 (1980)
4. Braun, J.: The many surface expressions of mantle dynamics. Nature Geosc. **3**, 825–833 (2010)
5. Cathles, L.M.: The Viscosity of the Earth's Mantle. Princeton Univ. Press, Princeton (1975)
6. Cazenave, A., Nerem, R.S.: Present-day sea level change: Observations and causes. Rev. Geophys. **42**(RG3001) (2004)
7. Ekman, M.: The World's longest continued series of sea-level observations. Pure Appl. Geophys. **127**, 73–77 (1988)
8. England, P.C., Houseman, G.A.: Finite strain calculations of continental deformation II. Comparison with the India-Asia collision zone. J. Geophys. Res. **91**, 3664–3676 (1986)
9. Farrell, W., Clark, J.A.: On postglacial sea level. Geophysical Journal of the Royal Astronomical Society **46**(3), 647–667 (1976)
10. Forte, A.M., Peltier, W.R., Dziewoński, A.M.: Inferences of mantle viscosity from tectonic plate velocities. Geophys. Res. Lett. **18**, 1747–1750 (1991)
11. Haskell, N.A.: The motion of a viscous fluid under a surface load. Physics **6**, 265–269 (1935)
12. Haskell, N.A.: The motion of a viscous fluid under a surface load, part 2. Physics **7**, 56–61 (1936)
13. Johansson, J.M., Davis, J.L., Scherneck, H.G., Milne, G.A., Vermeer, M., Mitrovica, J.X., Bennett, R.A., Jonsson, B., Elgered, G., Elosegui, P., Koivula, H., Poutanen, M., Ronnang, B.O., Shapiro, I.: Continuous GPS measurements of postglacial adjustment in fennoscandia – 1. Geodetic results. J. Geophys. Res. **107**, 2157 (2002)
14. Johnson, A.M., Fletcher, R.C.: Folding of Viscous Layers. Columbia University Press (1994)
15. King, S.D.: Archean cratons and mantle dynamics. Earth Planet. Sci. Lett. **234**, 1–14 (2005)
16. King, S.D.: Reconciling laboratory and observational models of mantle rheology in geodynamic modeling. J. Geodyn. **100**, 33–50 (2016)
17. King, S.D., Anderson, D.L.: Edge driven convection. Earth Planet. Sci. Lett. **160**, 289–296 (1998)
18. Lambeck, K., Yokoyama, Y., Johnston, P., Purcell, A.: Global ice volumes at the Last Glacial Maximum and early lateglacial. Earth Planet. Sci. Lett. **181**, 513—-527 (2000)
19. Landerer, F.W., Swenson, S.C.: Accuracy of scaled GRACE terrestrial water storage estimates. Water Resource Res. **48**(W04531) (2012). doi:10.1029/2011WR011453
20. Love, A.E.H.: The stress produced in a semi-infinite solid by pressure on part of the boundary. Phil. Tran. Roy. Soc. London, Ser. A **228**, 377–379 (1929)
21. Mazzotti, S., Lambert, A., Henton, J., James, T.S., Courtier, N.: Absolute gravity calibration of GPS velocities and glacial isostatic adjustment in mid-continent North America. Geophys. Res. Lett. **38**(L24311) (2011). doi:10.1029/2011GL049846
22. Milne, G.A., Davis, J.L., Mitrovica, J.X., Scherneck, H.G., Johansson, J.M., Vermeer, M., Koivula, H.: Space-geodetic constraints on glacial isostatic adjustment in Fennoscandia. Science **291**, 2381–2385 (2001)
23. Milne, G.A., Mitrovica, J.X., Scherneck, H.G.: Estimating past continental ice volume from sea-level data. Quat. Sci. Rev. **21**, 361–376 (2002)
24. Mitrovica, J.X., Milne, G.A.: On post-glacial sea level: I. general theory. Geophys. J. Int. **154**, 253—-267 (2003)
25. Mitrovica, J.X., Tamisiea, M.E., Davis, J.L., Milne, G.A.: Recent mass balance of polar ice sheets inferred from patterns of global sea-level change. Nature **409**, 1026—-1029 (2001)
26. Morgan, W.J.: Rises, trenches, great faults, and crustal blocks. J. Geophys. Res. **73**, 1959–1982 (1968)

27. Nocquet, J.M., Calais, E., B., P.: Geodetic constraints on glacial isostatic adjustment in Europe. Geophys. Res. Lett. **32**(L06308) (2005)
28. Nygård, A., Sejrup, H.P., Haflidason, H., Bryn, P.: The glacial North Sea fan, southern Norwegian Margin: Architecture and evolution from the upper continental slope to the deep-sea basin. Marine and Petroleum Geology **22**(71–84) (2005)
29. Park, K.D., Nerem, R.S., Davis, J.L., Schenewerk, M.S., Milne, G.A., Mitrovica, J.X.: Investigation of glacial isostatic adjustment in the northeast US using GPS measurements. Geophys. Res. Lett. **29**, 1509–1512 (2002)
30. Parsons, B., Sclater, J.G.: An analysis of the variation of ocean floor bathymetry and heat flow with age. J. Geophys. Res. **82**, 803–827 (1977)
31. Paulson, A., Zhong, S., Wahr, J.: Modelling post-glacial rebound with lateral viscosity variations. Geophys. J. Int. **163**, 357–371 (2005)
32. Peltier, W.: Impulse response of a Maxwell Earth. Rev. Geophys. **12**, 649–669 (1974)
33. Peltier, W., Argus, D., Drummond, R.: Space geodesy constrains ice-age terminal deglaciation: The global ICE-6G_C (VM5a) model. J. Geophys. Res. **120**, 450–487 (2015)
34. Peltier, W., Tushingham, A.M.: Influence of glacial isostatic-adjustment on tide-gauge measurements of secular sea-level change. J. Geophys. Res. **96**, 6779—-67,960 (1991)
35. Ramillien, G., Bouhours, S., Lombard, A., Cazenave, A., Flechtner, F., Schmidt, R.: Land water storage contribution to sea level from GRACE geoid data over 2003–2006. Global Planet. Change **60**, 381—-392 (2008)
36. Schubert, G., Turcotte, D.L., Olson, P.: Mantle Convection in the Earth and Planets. Cambridge University Press (2001)
37. Sella, G.F., Dixon, T.H., Mao, A.: REVEL: A model for recent plate velocities from space geodesy. J. Geophys. Res. **107** (2002). doi:10.1029/2000JB000033
38. Sella, G.F., Stein, S., Dixon, T.H., Craymer, M., James, T.S., Mazzotti, S., Dokka, R.K.: Observation of glacial isostatic adjustment in "stable" North America with GPS. Geophys. Res. Lett. **34**(L02306) (2007). doi:10.1029/2006GL027081
39. Spada, G., Antonioli, A., Cianetti, S., Giunchi, C.: Glacial isostatic adjustment and relative sea-level changes: the role of lithospheric and upper mantle heterogeneities in a 3-d spherical earth. Geophys. J. Int. **165**, 692–702 (2006)
40. Tamisiea, M.E., Mitrovica, J.X., Davis, J.L.: GRACE gravity data constrain ancient ice geometries and continental dynamics over Laurentia. Science **5826**, 881–883 (2007)
41. Tamisiea, M.E., Mitrovica, J.X., Milne, G.A., Davis, J.L.: Global geoid and sea level changes due to present-day ice mass fluctuations. J. Geophys. Res. **106**, 30,849–30,863 (2001)
42. van Veen, J.: Bestaat er een geologische bodemdaling te Amsterdam sedert 1700? Tijdschrift Koninklijk Nederlandsch Aardrijkskundig Genootschap **2: LXII** (1945)
43. Wang, H., Wu, P.: Effects of lateral variations in lithospheric thickness and mantle viscosity on glacially-induced surface motion on a spherical, self-gravitating Maxwell Earth. Earth Planet. Sci. Lett. **244**, 576–589 (2006)
44. Wilson, J.T.: Did the Atlantic close and then reopen? Nature **211**, 676–681 (1966)
45. Wu, P.: Mode coupling in a viscoelastic self-gravitating spherical earth induced by axisymmetric loads and lateral viscosity variations. Earth Planet. Sci. Lett. **197**, 1–10 (2002)